Desalination and Water Treatment
www.deswater.com

doi: 10.5004/dwt.2023.29400

287 (2023) 89–95
March

Application of Box–Behnken experimental design to ultrafiltration of olive oil mill wastewater

Ezgi Oktav Akdemir

Department of Environmental Engineering, Engineering Faculty, Dokuz Eylul University, Tinaztepe Campus, 35160 Buca – Izmir, Turkey, email: ezgi.oktav@deu.edu.tr

Received 27 September 2022; Accepted 11 February 2023

ABSTRACT

In this study, an ultrafiltration process was used for olive oil mill wastewater pretreatment. Chitosan was used to increase the efficiency of the ultrafiltration process. The Box–Behnken statistical experiment design method was used to determine the effects of operating parameters such as chitosan concentration, feed flowrate and ultrafiltration time on permeate flux and percent chemical oxygen demand (COD) removal. The response function coefficients were calculated using the Design-Expert 7.0 program. The predicted values of permeate flux and COD removal efficiency obtained using the response function were in good agreement with the experimental data. The permeate flux increased with the increase in flow rate and decreased with the increase in chitosan concentration. The decline in flux was not significant during the whole filtration period. So, the optimum set of chitosan concentration and feed flowrate for permeate flux was 100 mg/L and 200 L/h, respectively, with 43 L/m^2·h flux value at 30 min operation time. On the other hand, COD removal efficiency decreased with increasing flow rate and increased with increasing chitosan concentration. The optimal set was 600 mg/L and 100 L/h for COD removal, with 80% COD removal efficiency at 80 min of ultrafiltration time.

Keywords: Box–Behnken experimental design; Chitosan; Chemical oxygen demand; Olive oil mill wastewater; Permeate flux

1. Introduction

The main products obtained from olive trees are table olives and olive oil, which are essential components of a healthy nutrition. In olive oil production facilities, olive washing waters and olive vegetation waters containing high amounts of pollution are mixed together and labeled as olive mill wastewater (OMW) [1]. OMW is one of the most important industrial wastewaters in the Mediterranean countries due to its high organic load and phenolic compounds [2].

The OMW is characterized by high concentrations of several organic compounds, such as organic acids, sugars, tannins, and phenolic compounds [3]. In addition to all this, OMW has an acidic pH, high electrical conductivity, high salinity, and above all lipidic and phenolic fractions, organic long chain fatty acids, tannins and organohalogenated contaminants [4]. These ingredients make OMW difficult to treat.

OMW is usually directly discharged into surface waters or stored in evaporation ponds. However, these ponds can pollute groundwater and cause other environmental problems. A lot of research has been done on the development of efficient technologies for the treatment of OMW. These technologies are physical, chemical, biological or combined technologies, including aerobic and anaerobic digestion [5], flocculation, sedimentation [6], evaporation [7], electrocoagulation [8], advanced oxidation processes such as ozonation [9], Fenton's reagent, electrochemical oxidation [10], and membrane processes [11,12].

The statistical models have been found to be useful for the optimization of different parameters in removing pollutants from wastewaters. One of these statistical models for experimental design is the response surface methodology (RSM). The lower number of trials, interactions of variables, determination of optimal theoretical conditions, and the final elimination formula have been advantageous [13]. The nature of the final elimination formula will be illustrated in the results section. The response surface methodology for experimental designs includes a three-level factorial design, central composite design (CCD), a D-optimal design, and a Box–Behnken design [14]. Among all these experimental designs, the Box–Behnken design is a modified central compound experimental design with excellent predictability [15]. Not only does it require less experimentation than other RSM designs with the same number of factors, but it is also more efficient than CCD and three-level factorial designs.

The aim of the present work was to investigate the treatment of OMW by ultrafiltration membrane. The ultrafiltration system was preferred due to its lower pressure and energy requirement compared to the nanofiltration process. In addition, it is predicted that chemical oxygen demand (COD) removal efficiencies in treated water will be higher than microfiltration membranes. Chitosan was used to increase the efficiency of the ultrafiltration process. Box–Behnken design (3 factors and 3 levels) was employed to investigate the effect of chitosan concentration, flow rate, and ultrafiltration time on the removal efficiency of the ultrafiltration process on olive oil mill wastewater. The optimal conditions for maximizing either permeate flux and/or COD removal efficiency were determined in the content of this work.

2. Materials and methods

2.1. Olive oil mill wastewater and chitosan

A sample of olive oil mill wastewater was obtained from a 3-phase continuous olive oil mill plant located in Izmir (Turkey). A sample was collected in December from the effluent of the horizontal decanter. A fresh sample was kept in the dark at 4°C.

Chitosan was taken from Sigma-Aldrich (product number 419419) with a high molecular weight. During membrane experiments, chitosan at the determined doses was weighed and added to the feed vessel.

2.2. Membrane experiments

The membrane experiments were carried out in a laboratory-scale cross flow membrane system. The feed stream was pumped from the feed vessel to the feed inlet of the cell body. A portion of the solution permeated through the membrane and flowed into the permeate carrier. The concentrate stream flowed back to the feed vessel. A cooling system with tap water in the feed vessel was used in all filtration experiments to keep the temperature at 22°C–24°C. A 5 mm cartridge filter was used before the ultrafiltration membrane as a prefilter. Osmonics Sepa CF II membrane system described in detail in our previous works [12,16] has also been used in this study. At the beginning of the experiments, chitosan was added in the determined quantities to raw olive mill wastewater, and this wastewater was filled into the feed vessel of the experimental set-up. The permeate from the membrane was collected in the permeate collection vessel. The pressure and the recycle flow rate were controlled by regulation valves. During the filtration experiments, the mass of permeate in the permeate carrier was continuously monitored. During the filtration experiments, the mass of permeate in the permeate carrier was continuously monitored. A schematic flow diagram of the experimental set-up is given in Fig. 1. The MW ultrafiltration membrane from Osmonics with a molecular weight cut-off of 100 kDa was used in this study. Membrane was washed after each experiment and kept overnight in a solution of isopropanol/water (1:1 v/v) containing hypochlorite of sodium to remove eventual coloration caused by the treated effluents. Membrane area was 0.0155 m^2 for all membrane experiments.

2.3. Experimental design

Box–Behnken design was applied in this study as the response surface methodology (RSM) tool because Box–Behnken design needs fewer runs than all the other RSM designs. This design allows and shows to efficiency at intermediate levels not experimentally studied.

The mathematical relationship that is offered by the Box–Behnken design application between the dependent variables (Y) and the independent variables (X) can be approximated by a (second-order) polynomial equation as follows:

$$Y = b_0 + \underbrace{\sum b_i X_i}_{\text{linear}} + \underbrace{\sum b_{ij} X_i X_j}_{\text{interaction}} + \underbrace{\sum b_{ii} X_i^2}_{\text{squared}} \quad (1)$$

where Y is the predicted response, b_0 is offset term, b_i is the linear effect while b_{ii} and b_{ij} are the square and the interaction effects, respectively. This approach was selected to predict a potential response function. A total of 15 experiments are required to determine the 9 coefficients of the quadratic equation. This regression model includes one block term, three linear terms, three quadratic terms, and three interaction terms.

The Box–Behnken statistical experiment design method was used to determine the effects of operating parameters on permeate flux and COD removal efficiency. Three important operating parameters; chitosan concentration (X_1), flow rate (X_2) and ultrafiltration time (X_3) were considered independent variables. Preliminary experiments were made to determine the experimental points, and using the results obtained from this, the chitosan concentration (CC, X_1) was

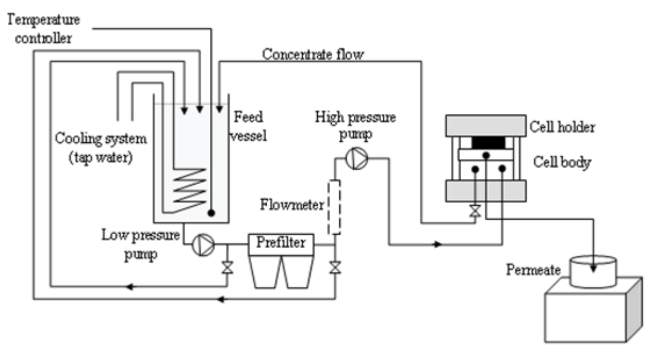

Fig. 1. Schematic flow diagram of the experimental set-up.

chosen between 100 and 600 mg/L, the flow rate (FR, X_2) was between 100–200 L/h, and the ultrafiltration time (UT, X_3) was between 30 and 20 min. The response function coefficients were calculated using the Design-Expert 7.0 program. The low, center and high levels of each variable organized by statistical approach as –1, 0, and +1, respectively are shown in Table 1.

3. Results and discussions

3.1. Characterization of olive mill wastewaters

A sample of OMW was taken from a 3-phase olive oil production plant. The main physicochemical characteristics of the used OMW are given in Table 2. OMW has a dark brown color and a characteristic smell.

3.2. Box–Behnken experimental design method results

The experimental conditions that are performed according to the Box–Behnken design are given in Table 3. Obtained results at the predetermined runs planned by Box–Behnken are also presented in the same table. After experiments, predicted results are determined by Box–Behnken statistical approach at the predetermined experimental runs. In order to, compare observed and predicted results, all experimental and predicted results are presented in Table 4.

The effects of each parameter on permeate flux and COD removal by means of a regression model can be shown in Eqs. (2) and (3). It can be said that chitosan concentration and filtration time had a decreasing effect, and flow rate had an increasing effect on permeate flux. On the contrary, the increase in chitosan concentration and ultrafiltration time increases the COD removal efficiency, while the increase in flow rate decreases the COD removal efficiency.

$$\begin{aligned} Y_1 = {} & +56.27416 - 0.10602X_1 + 0.035140X_2 - 0.19923X_3 \\ & + 0.000023X_1X_2 + 0.0000381X_1X_3 + 0.000157X_2X_3 \\ & + 0.000104X_1^2 + 0.000255X_2^2 + 0.00073X_3^2 \end{aligned} \tag{2}$$

$(R^2 = 0.996)$

$$\begin{aligned} Y_2 = {} & 61.79071 + 0.011578_{X_1} - 0.020109X_2 + 0.13898X_3 \\ & + 0.000001X_1X_2 + 0.0000958X_1X_3 + 0.000001X_2X_3 \\ & + 0.0000496X_1^2 - 0.0000388X_2^2 + 0.000864X_3^2 \end{aligned} \tag{3}$$

$(R^2 = 0.999)$

Table 1
Levels of each factor for Box–Behnken experimental design

Independent factors	Symbol	Coded levels		
		–1	0	+1
Chitosan concentration, mg/L	X_1	100	350	600
Flowrate, L/h	X_2	100	150	200
Ultrafiltration time, min	X_3	30	75	120

Table 2
Characterization of raw olive oil mill wastewaters

Parameter	Value
pH	5.4
Five-day biochemical oxygen demand, mg/L	36,360
Chemical oxygen demand, mg/L	120,000
Total organic carbon, mg/L	31,650
Suspended solids, mg/L	33,200
Oil and grease, mg/L	3,070
Phenolics, mg/L	9,322

Table 3
Results of the Box–Behnken experiments at the predetermined experimental points

Run	Actual and coded levels of variables			Experimental results	
	X_1 Chitosan concentration (mg/L)	X_2 Flowrate (L/h)	X_3 Ultrafiltration time (min)	Y_1 Permeate flux (L/m²·h)	Y_2 Chemical oxygen demand removal (%)
1	100 (–1)	100 (–1)	75 (0)	35.3	65.1
2	600 (+1)	100 (–1)	75 (0)	20.1	80.8
3	100 (–1)	200 (+1)	75 (0)	41.2	62.1
4	600 (+1)	200 (+1)	75 (0)	24.6	77.7
5	100 (–1)	150 (0)	30 (–1)	43.3	60.8
6	600 (+1)	150 (0)	30 (–1)	24.3	73.9
7	100 (–1)	150 (0)	120 (+1)	37.2	62.5
8	600 (+1)	150 (0)	120 (+1)	20.2	80.0
9	350 (0)	100 (–1)	30 (–1)	25.9	65.9
10	350 (0)	200 (+1)	30 (–1)	28.9	62.5
11	350 (0)	100 (–1)	120 (+1)	20.7	69.7
12	350 (0)	200 (+1)	120 (+1)	25.2	66.4
13	350 (0)	150 (0)	75 (0)	23.0	68.7
14	350 (0)	150 (0)	75 (0)	23.0	68.6
15	350 (0)	150 (0)	75 (0)	23.1	68.7

The analysis of variance (ANOVA) results are presented in Tables 5 and 6. An ANOVA is employed to determine the statistical significance of all analyses. The statistical significance of quadratic fit is determined by the lack of fit (LOF), coefficient of determination (R^2), and adjusted coefficient of determination (R^2 adj.) between the predicted and experimental values. Tables 5 and 6 indicate that the *p*-value of the presented model is lower than 0.0001. It is approved that all the parameters are significant and that the used model can be an efficient model for the prediction of experimental values. The model *F*-ratio of 140.27 for permeate flux and 3,048.98 for COD removal implies that the model is significant. Another parameter is lack of fit. If the *p*-value is lower than 0.05, it can be considered a significant model. According to Tables 5 and 6, the *p*-value (lower than 0.0001) is significant for permeate flux and COD removal, which indicates the conformity of the presented model. Also, R^2 and R^2 adj. values are estimated to be 0.9961 and 0.9890 for permate flux, 0.9998 and 0.9995 for COD removal, respectively. A higher value of them indicates that the model is absolutely consistent with the experimental results.

Table 4
Observed and predicted values for the response functions

Run number	Permeate flux (L/m²·h)		Chemical oxygen demand removal efficiency (%)	
	Observed	Predicted	Observed	Predicted
1	35.3	35.7	65.1	65.3
2	20.1	20.0	80.8	80.7
3	41.2	41.1	62.1	62.3
4	24.6	24.2	77.7	77.4
5	43.3	42.9	60.8	59.9
6	24.3	24.9	73.9	74.1
7	37.2	37.6	62.5	62.6
8	20.2	20.1	80.0	79.7
9	25.9	25.4	65.9	65.8
10	28.9	29.7	62.5	63.1
11	20.7	20.8	69.7	69.8
12	25.2	24.9	66.4	66.4
13	23.0	23.1	68.7	68.7
14	23.0	23.1	68.6	68.7
15	23.1	23.1	68.7	68.7

3.3. Variation of permeate flux

In the first part of the experimental studies, effects of chitosan concentration, flow rate, and ultrafiltration time on the permeate flux were investigated, and the results are given in Fig. 2a–c.

As it can be seen from Fig. 2a and c, permeate flux increased with increasing feed flow rate. The feed flow rate parameter determines the tangential crossflow velocity. An increase in the cross-flow velocity results in an increase in the forced convection of the solutes, enhancing their transport from the membrane surface to the bulk feed. This reduces the concentration polarization and increases the permeate flux [16–18]. In this study, permeate flux increases are significantly associated with increasing flow rate. Therefore, operating at the maximum flow rate seems reasonable.

Variation of permeate flux with the chitosan concentration can be seen from Fig. 2a at different flow rate and Fig. 2b at different operation time. The increase in the concentration of chitosan causes a decrease in permeate flux. At a 100 L/h flow rate, the flux obtained at a 100 mg/L of chitosan concentration was 35.3 L/m²·h, while at a 600 mg/L chitosan concentration, this value dropped to 20.1 L/m²·h. Similar results are seen in the graphs of ultrafiltration time and chitosan change. When the 30-min ultrafiltration time results were examined, the flux at the concentration of 100 mg/L chitosan was 42.9 L/m²·h while the flux decreased to 24.3 L/m²·h when the chitosan concentration increased to 600 mg/L. As the

Table 5
Analysis of variance test for the response function Y_1 (permeate flux)

Source	Sum of squares	d.f.	Mean square	*F*-ratio	*p*-value
Model	814.72	9	90.52	140.27	<0.0001
X_1 (chitosan conc.)	566.18	1	566.18	877.29	<0.0001
X_2 (flowrate)	40.23	1	40.23	62.33	0.0005
X_3 (ultrafiltration time)	46.36	1	46.36	71.83	0.0004
X_1X_2	0.34	1	0.34	0.53	0.4997
X_1X_3	0.74	1	0.74	1.14	0.3339
X_2X_3	0.50	1	0.50	0.78	0.4184
X_1^2	156.89	1	156.89	243.10	<0.0001
X_2^2	1.50	1	1.50	2.32	0.1885
X_3^2	7.96	1	7.96	12.34	0.0171
Residual	3.23	5	0.65		
Lack of fit	3.23	3	1.08		
Pure error	0.000	2	0.000		
Cor. total	817.95	14			

R-squared = 0.9961, *R*-squared (adjusted for df) = 0.9890.

Table 6
Analysis of variance test for the response function Y_2 (chemical oxygen demand removal)

Source	Sum of squares	d.f.	Mean square	F-ratio	p-value
Model	563.69	9	62.63	3,048.98	<0.0001
X_1 (chitosan conc.)	458.78	1	458.78	22,333.89	<0.0001
X_2 (flowrate)	20.14	1	20.14	980.59	<0.0001
X_3 (ultrafiltration time)	29.90	1	29.90	1,455.72	<0.0001
X_1X_2	0.000	1	0.000	0.000	1.000
X_1X_3	4.64	1	4.64	226.11	<0.0001
X_2X_3	0.000	1	0.000	0.000	1.000
X_1^2	35.41	1	35.41	1,723.88	<0.0001
X_2^2	0.035	1	0.035	1.69	0.2506
X_3^2	11.29	1	11.29	549.69	<0.0001
Residual	0.10	5	0.021		
Lack of fit	0.10	3	0.034		
Pure error	0.000	2	0.000		
Cor. total	563.79	14			

R-squared = 0.9998, R-squared (adjusted for df) = 0.9995.

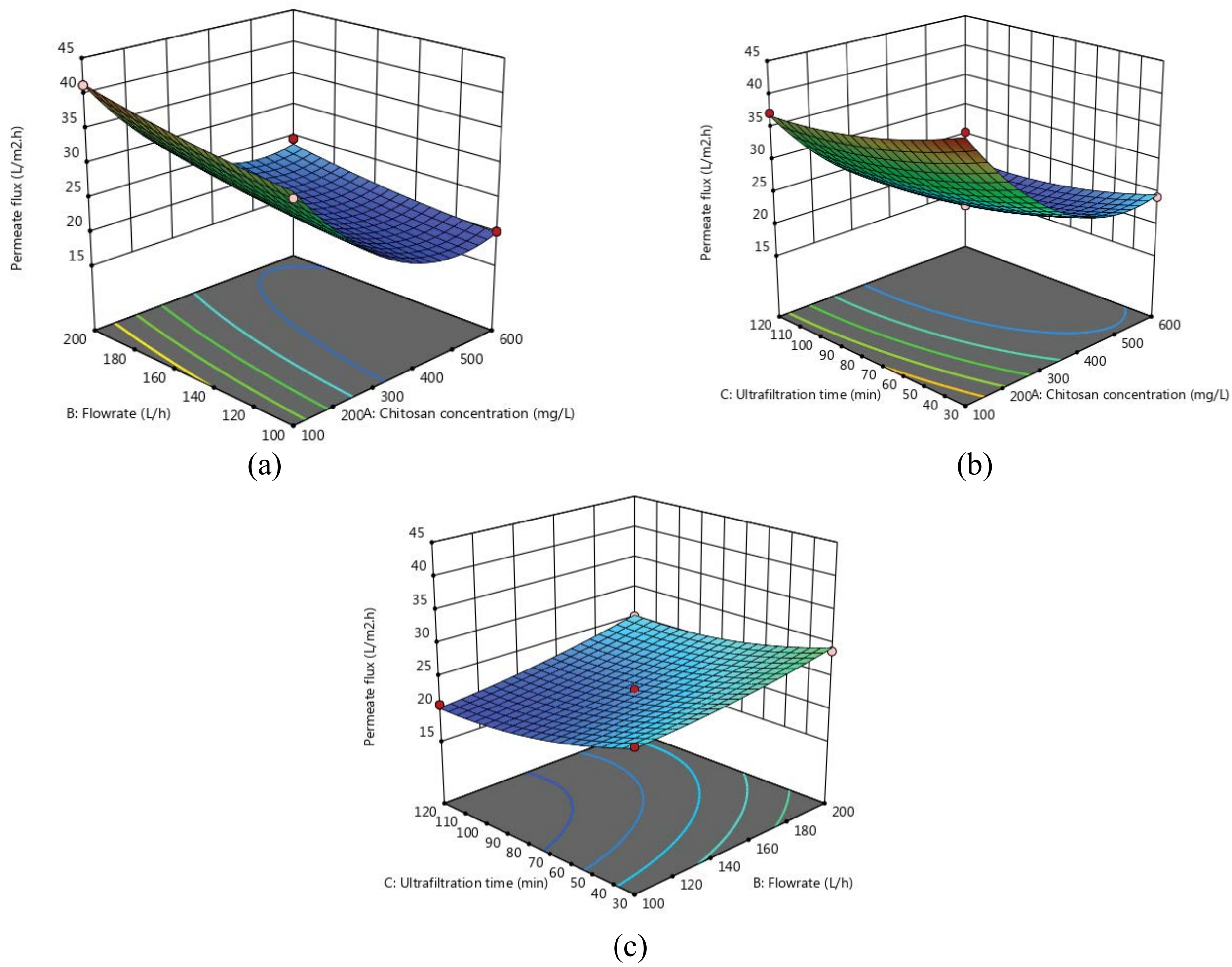

Fig. 2. Variation of permeate flux with (a) flow rate and chitosan concentration at 75 min ultrafiltration time, (b) ultrafiltration time and chitosan concentration at 150 L/h flowrate and (c) ultrafiltration time and flowrate, and at 350 mg/L chitosan concentration.

concentration of chitosan added to the OMW increases, the membrane surface is covered with chitosan, in which case the flux value is reduced [12].

Variations of permeate flux as a function of ultrafiltration time at different chitosan concentrations and flow rates are given in Fig. 2b and c. As it can be seen from the figures, permeate flux showed the same trend for all flow rates and chitosan concentrations. The descending rate of flux is not significant during the whole filtration period. After about 75 min of ultrafiltration time, flux reaches a more or less constant value because the cake layer reaches equilibrium and its growth ceases after this time. So, the cake layer resistance and subsequent permeate flux remain constant [12,19].

As results of all ultrafiltration experiments, maximum permeate flux was obtained at 100 mg/L chitosan concentration, 200 L/h feed flow rate and 30 min ultrafiltration time as 43 L/m²·h.

3.4. Variation of COD removal

In the second part of the experimental studies, the effects of chitosan concentration, flow rate, and ultrafiltration time on the COD removal efficiency were investigated. The effects of the flow rate on the COD removal efficiency are given in Fig. 3a and c. As it can be seen from those two figures, COD removal efficiency decreases with increasing flow rate. It is because of turbulence due to increasing cross flow velocity or feed flow rate. Increasing turbulence reduces membrane fouling. Lower fouling increases the permeate flux through the membrane and decreases the removal efficiencies. This effect was also reported by other authors [16,20]. As seen in Fig. 3c, when chitosan is kept at 350 mg/L and the ultrafiltration time is kept constant for 30 min, the COD removal efficiency for a 100 L/h flowrate is 80%, whereas when the flowrate reaches 200 L/h, the efficiency decreases to 60%.

The influence of chitosan concentration on the COD removal efficiency at different flow rates and ultrafiltration times is depicted in Fig. 3a and b. The increase in chitosan concentration also increases COD removal efficiency. In experimental studies carried out at 100 L/h flow rate and 75 min of ultrafiltration time, the efficiency, which was 65% at 100 mg/L chitosan concentration, increased to 80% when chitosan was increased to 600 mg/L. Rizzo et al. [6] worked on the pretreatment of OMW by coagulation with chitosan,

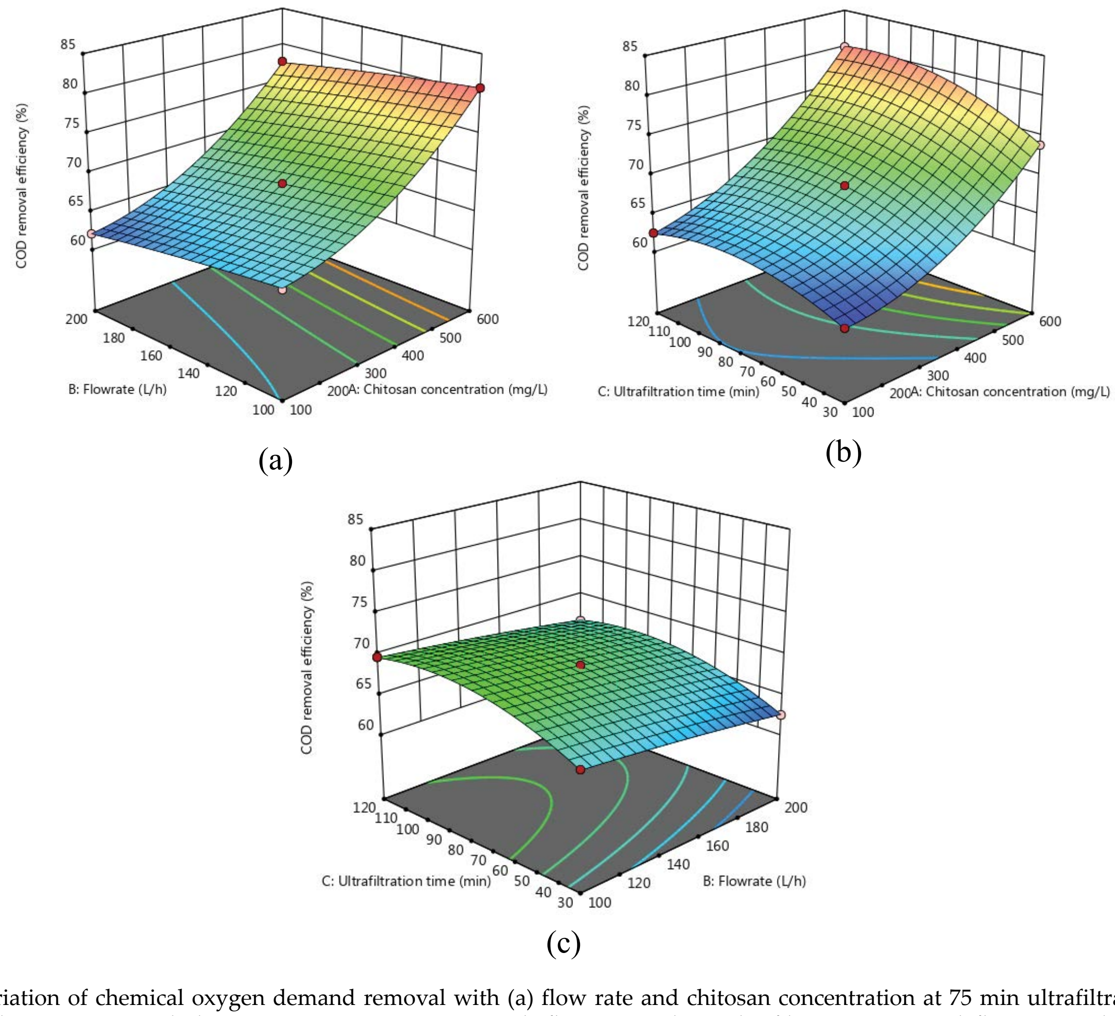

Fig. 3. Variation of chemical oxygen demand removal with (a) flow rate and chitosan concentration at 75 min ultrafiltration time, (b) ultrafiltration time and chitosan concentration at 150 L/h flowrate and (c) ultrafiltration time and flowrate with 350 mg/L chitosan concentration.

and they found a 32% COD removal efficiency as the optimum efficiency for a 400 mg/L chitosan dose. In our study, 70% COD removal efficiency was obtained for a 400 mg/L chitosan dose at a 100 L/h flowrate and 120-min ultrafiltration time.

The variation of COD removal efficiency with ultrafiltration time as a function of chitosan concentration is given in Fig. 3b, and as a function of flowrate, it is given in Fig. 3c. An increase in COD removal efficiencies occurred during the first 80 min of operation for all flowrates studied in this study. After 80 min, more or less steady state conditions were reached. After this period, no significant change was observed in COD removal efficiencies. As it can be seen from Fig. 3c, COD removal efficiency was 65% after 30 min, 69% after 80 min, and 70% after 120 min of operation at a 100 L/h flowrate. This result is similar to our previous works with the same wastewater [12,16].

4. Conclusions

A Box–Behnken statistical experimental design was used to determine the optimization of operating parameters such as chitosan concentration, feed flow rate, and ultrafiltration time on the permeate flux and COD removal efficiency for ultrafiltration of OMW.

In the Box–Behnken statistical experimental design, response function coefficients were determined by regression analysis of the experimental data, and predicted results obtained from the response functions were in good agreement with the experimental results. The correlation coefficients (R^2) between the observed and predicted values were 0.9961 and 0.9998 for permeate flux and COD removal, respectively. These results indicated excellent agreement between the observed and predicted values, indicating the reliability of the methodology used.

The optimum set for permeate flux was 100 mg/L chitosan concentration, 200 L/h feed flow rate, and 30 min of ultrafiltration time with a 43 $L/m^2 \cdot h$ flux value. On the other hand, the optimum set for COD removal was 600 mg/L chitosan concentration, 100 L/h feed flow rate, and 80 min of ultrafiltration time with 80% COD removal efficiency.

Since optimum sets are just at opposite corners of the operation region (chitosan concentration, flow rate), first of all the objective (COD removal or permeate flux) should be determined, and then optimum operation parameters can be selected. In addition, more pilot-scale experiments are needed so that the results obtained in this laboratory-scale study can be applied to full-scale units.

References

[1] S. Vuppala, I. Bavasso, M. Stoller, L Palma, Olive mill wastewater integrated purification through pre-treatments using coagulants and biological methods: experimental, modelling and scale-up, J. Cleaner Prod., 236 (2019) 117–122.

[2] A. Yazdanbakhsh, F. Mehdipour, A. Eslami, H.S. Maleksari, F. Ghanbari, The combination of coagulation, acid cracking and Fenton-like processes for olive oil mill wastewater treatment: phytotoxicity reduction and biodegradability augmentation, Water Sci. Technol., 71 (2015) 1097–1105.

[3] E. Turano, S. Curcio, M. De Paola, V. Calabrò, G. Iorio, An integrated centrifugation–ultrafiltration system in the treatment of olive mill wastewater, J. Membr. Sci., 209 (2002) 519–531.

[4] J.M. Ochando-Pulido, S. Pimentel-Moral, V. Verardo, A. Martinez-Ferez, A focus on advanced physico-chemical processes for olive mill wastewater treatment, Sep. Purif. Technol., 179 (2017) 161–174.

[5] A. González-González, F. Cuadros, Effect of aerobic pretreatment on anaerobic digestion of olive mill wastewater (OMWW): an ecoefficient treatment, Food Bioprod. Proc., 95 (2015) 339–345.

[6] L. Rizzo, G. Lofrano, V. Belgiorno, Olive mill and winery wastewaters pre-treatment by coagulation with chitosan, Sep. Sci. Technol., 45 (2010) 2447–2452.

[7] V. Kavvadias, M.K. Doula, K. Komnitsas, N. Liakopoulou, Disposal of olive oil mill wastes in evaporation ponds: effects on soil properties, J. Hazard. Mater., 182 (2010) 144–155.

[8] F. Erraib, K. Ass, Optimization of electrocoagulation operating parameters for COD removal from olive mill wastewater: application of Box–Behnken design, Mediterr. J. Chem., 9 (2019) 212–221.

[9] S. Siorou, T.T. Vgenis, M.A. Dareioti, M.S. Vidali, I. Efthimiou, M. Kornaros, D.I. Vlastos, S. Dailianis, Investigation of olive mill wastewater (OMW) ozonation efficiency with the use of a battery of selected ecotoxicity and human toxicity assays, Aquat. Toxicol., 164 (2015) 135–44.

[10] N. Papastefanakis, D. Mantzavinosand, A. Katsaounis, DSA electrochemical treatment of olive mill wastewater on Ti/RuO_2 anode, J. Appl. Electrochem., 40 (2010) 729–737.

[11] M. Stoller, J.M. Ochando-Pulido, R. Field, On operating a nanofiltration membrane for olive mill wastewater purification at sub- and super-boundary conditions, Membranes, 7 (2017) 36, doi: 10.3390/membranes7030036.

[12] E.O. Akdemir, E. Aygan, Pretreatment of olive mill wastewater by ultrafiltration process using chitosan, Desal. Water Treat., 142 (2019) 49–55.

[13] K. Hasani, A. Peyghami, A. Moharrami, M. Vosoughi, A. Dargahi, The efficacy of sono-electro-Fenton process for removal of cefixime antibiotic from aqueous solutions by response surface methodology (RSM) and evaluation of toxicity of effluent by microorganisms, Arabian J. Chem., 13 (2020) 6122–6139.

[14] H. Zhang, Y.L. Li, X.G. Wu, Y.J. Zhang, D.B. Zhang, Application of response surface methodology to the treatment landfill leachate in a three-dimensional electrochemical reactor, Waste Manage., 30 (2010) 2096–2102.

[15] I. Grčić, D. Vujević, J. Šepčić, N. Koprivanac, Minimization of organic content in simulated industrial wastewater by Fenton type processes: a case study, J. Hazard. Mater., 170 (2009) 954–961.

[16] E.O. Akdemir, A. Ozer, Investigation of two ultrafiltration membranes for treatment of olive oil mill wastewater, Desalination, 249 (2009) 660–666.

[17] K. Auddy, S. De, S. Das Gupta, Flux enhancement in nanofiltration of dye solution using turbulent promoters, Sep. Purif. Technol., 40 (2004) 31–39.

[18] R.W. Field, J.J. Wu, On boundary layers and the attenuation of driving forces in forward osmosis and other membrane processes, Desalination, 429 (2018) 167–174.

[19] J.M. Ochando-Pulido, M. Stoller, L. Di Palma, P. Martínez-Ferez, On the optimization of a flocculation process as fouling inhibiting pretreatment on an ultrafiltration membrane during olive mill effluents treatment, Desalination, 393 (2016) 151–158.

[20] F.J. Benitez, J.L. Acero, A.I. Leal, Application of microfiltration and ultrafiltration processes to cork processing wastewaters and assessment of the membrane fouling, Sep. Purif. Technol., 50 (2006) 354–364.